35th WORLD VETERINARY ASSOCIATION CONGRESS
San José, Costa Rica | 27 - 30th April 2019

El equino como modelo para la investigación ortopédica traslacional. Ejemplos de estudios sobre la regeneración de cartílago y hueso realizados en Costa Rica

Expositor: PhD. Rafael Ángel Vindas Bolaños

Profesor de cirugía de especies mayores, especialista en equinos.
Decano de la Facultad de Ciencias de la Salud.

Universidad Nacional, Costa Rica

Rafael Vindas Bolaños PhD[1], René van Weeren PhD[3], Janny de Grauw PhD[3], Jos Malda, PhD[2]

[1]Cátedra de Cirugía de Especies Mayores, Universidad Nacional, Costa Rica
[2]Department of Orthopaedics University Medical Center Utrecht, The Netherlands
[3]Department of Equine Sciences Faculty of Veterinary Medicine, Utrecht University, The Netherlands

Otros colaboradores: en la anestesia inhalatoria Manuel Estrada McDermott y en apoyo logístico
Juan Manuel Estrada Umaña del Hospital de Equinos de la Universidad Nacional, Costa Rica.

WORLD VETERINARY ASSOCIATION

Agenda de la conferencia

1. Generalidades.
2. Métodos para fijación de matrices en defectos condrales u osteocondrales.
3. Modelo de la tuberosidad coxal del equino “in vivo” para estudios de regeneración de hueso y su aplicación al hueso subcondral.
4. Modelo de la rodilla del equino para estudios de regeneración de cartílago y hueso subcondral mediante defectos subcondrales.
5. Comparación entre un método de estimulación de la médula ósea y de un novedoso hidrogel auto adherible en defectos condrales de la rodilla del equino (in vivo) para estudios de regeneración de cartílago.
6. Conclusiones y agradecimientos.

1. Generalidades de cartílago, hueso subcondral y hueso y tipos de defectos para estudios de medicina regenerativa en cartílago.

Cell-free regenerative medicine (RM) strategies for cartilage and bone put to the test in the challenging equine in vivo model, Vindas Bolaños. R. (2019).

Generalidades

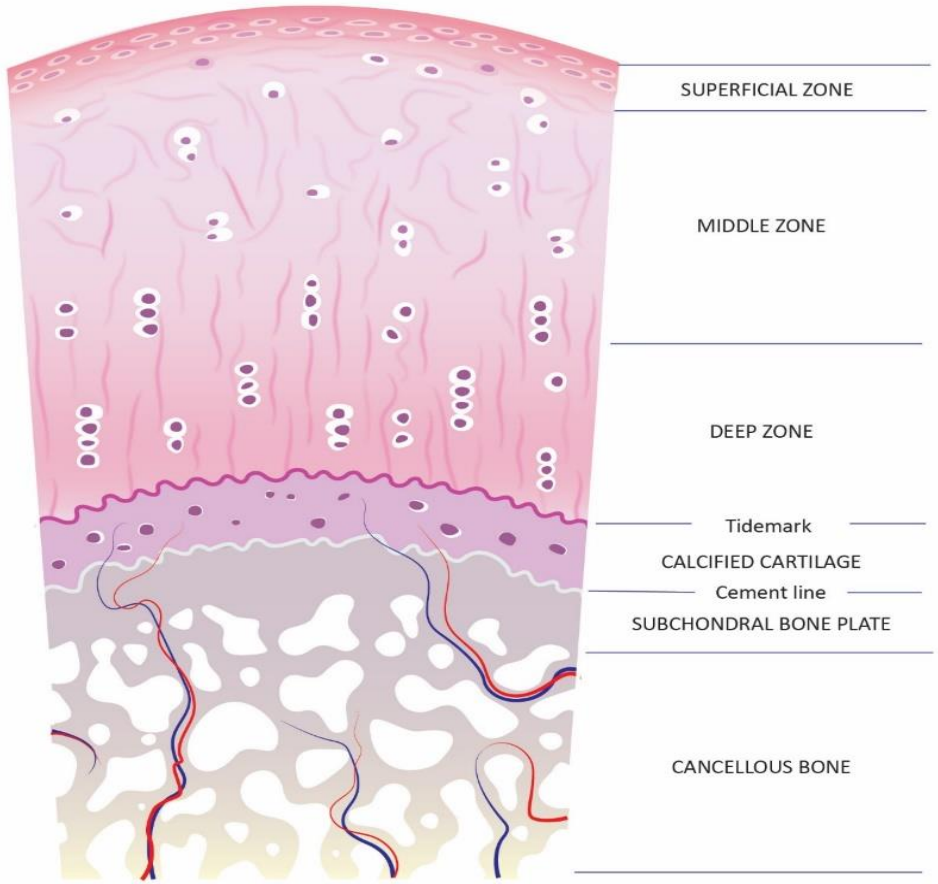

Schematic drawing of the structure of mature articular cartilage and subchondral bone. The tissue consists of a hyaline cartilage layer with three distinct zones: the superficial, middle and deep zone; the calcified cartilage layer and the subchondral bone.

Generalidades

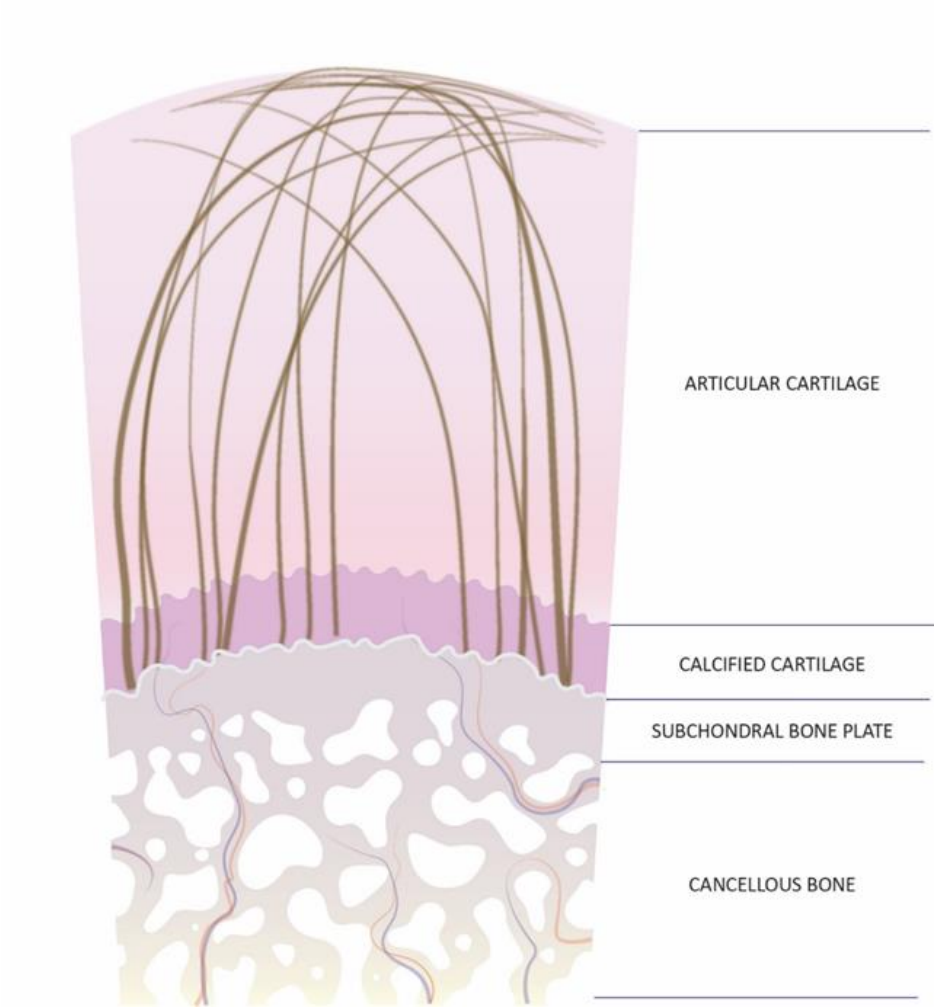

Schematic drawing of the arch-like configuration of the collagen fibers in articular cartilage. Fiber orientation in the superficial zone is tangential to the cartilage surface, in the deep zone perpendicular to it. In the middle zone the fibers describe an arc, resulting in an anisotropic configuration.

Generalidades

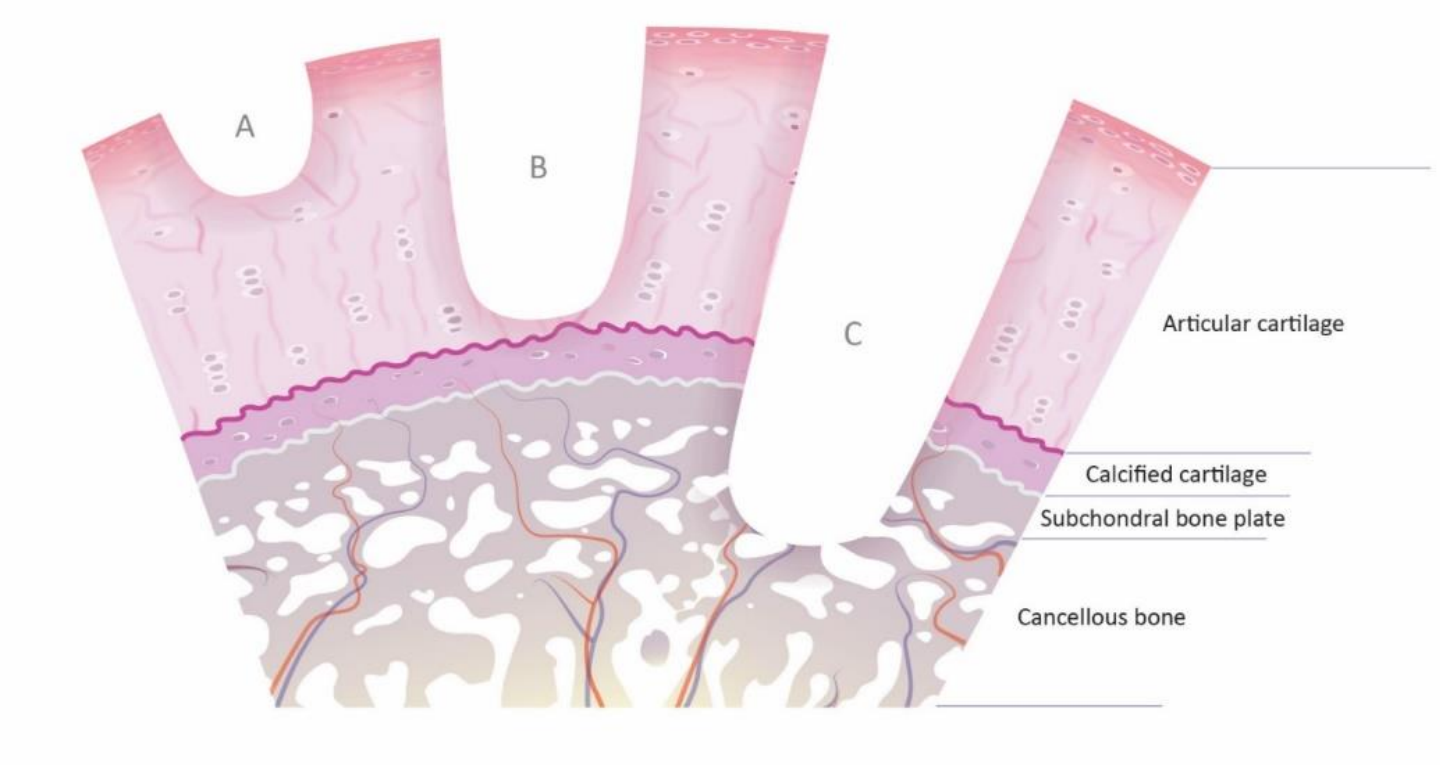

A. Partial thickness defect; B. Full thickness defect excluding the calcified cartilage layer; C. Osteochondral defect.

2. Métodos para fijación de matrices en defectos osteocondrales u condrales.

Fixation of hydrogel constructs for cartilage repair in the equine model: a challenging issue

Mancini, I.A.D., Vindas Bolaños, R.A., Brommer, H., Castilho, M., Ribeiro, A., van Loon, J.P.A.M., Mensinga, A., van Rijen, M.H.P., Malda, J., vanWeeren,P.R. (2017).

Fixation of hydrogel constructs for cartilage repair in the equine model: a challenging issue

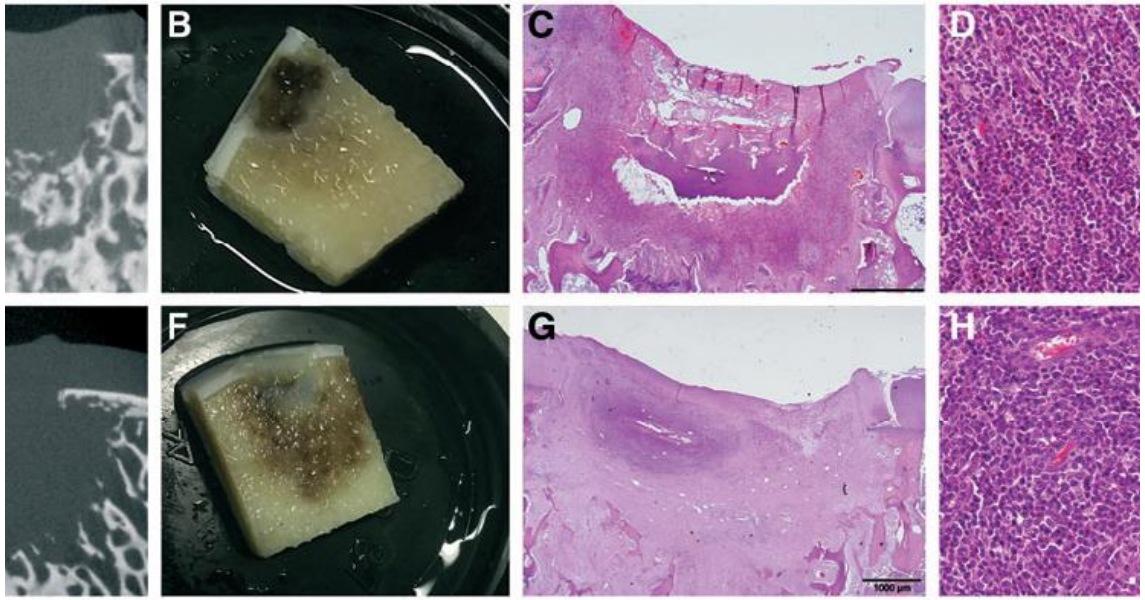

FIG. 4. Inflammatory reaction in control defects filled with CFG (14 days postoperatively). First and second rows show representative examples from two different animals. micro-CT imaging showed loss of the trabecular structure and bone resorption (A, E). Upon sectioning the bone loss was confirmed, and a reaction of the surrounding area with inflammation was visible to the naked eye (B, F). HE staining showed a focal reaction (C, G) with recruitment of neutrophil granulocytes with loss of architecture and bone structure (D, H). CFG, commercial fibrin glue; HE, hematoxylin and eosin.

Fixation of hydrogel constructs for cartilage repair in the equine model: a challenging issue

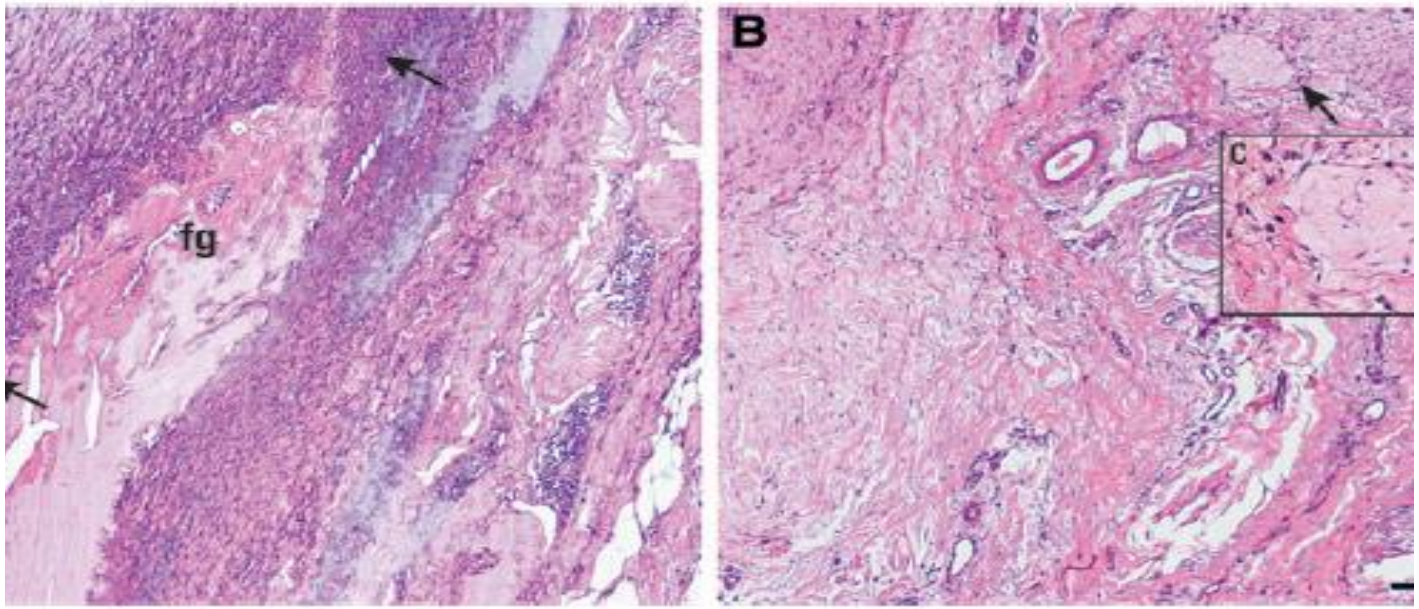

Histological sections of commercial (A, left) and autologous (B, right) fibrin glue, implanted in an equine ectopic model for 14 days. CFG appears contracted and is easily recognizable (A, fg); the glue is surrounded by a front of neutrophil granulocytes (A, black arrows); this is not present in the area where the autologous fibrin was implanted (B), where some macrophages and fibroblasts are present (C) (black bar = 200 m).

Fixation of hydrogel constructs for cartilage repair in the equine model: a challenging issue

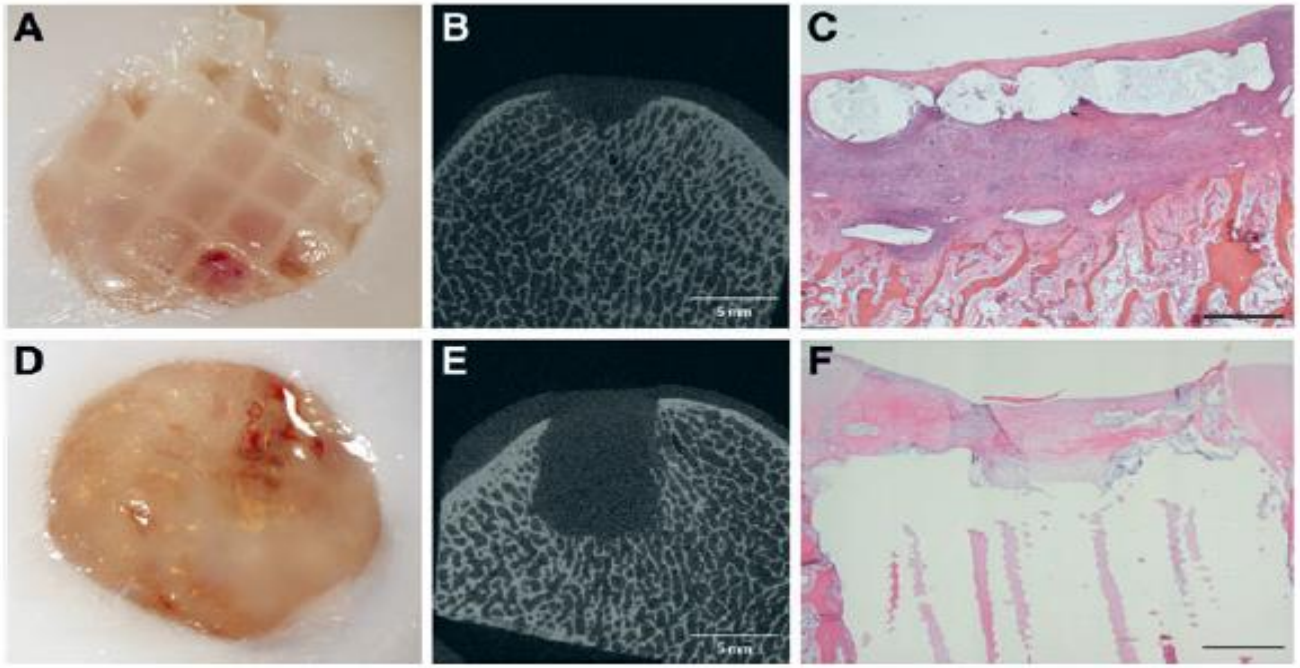

Fixation potential of two techniques, autologous fibrin glue (top) and PCL osteal anchor (bottom), 14 days after implantation. Reinforced chondral constructs appeared still in place in two of three cases; however, the scaffolds looked as if they were starting to slip out proximally (A). micro-CT of AFG fixation showed some bone resorption (B), confirmed by the HE staining (C), which showed loss of architecture directly underneath the defect with significant infiltration of neutrophil granulocytes and fibroblasts. Constructs fixated with the PCL anchor were all still in place (D), and micro-CT imaging showed a conserved trabecular architecture surrounding the construct (E). The chondral portion of the defect appears filled with repair tissue with a predominance of fibroblasts (F) (Black bar = 1mm).

Fixation of hydrogel constructs for cartilage repair in the equine model: a challenging issue

Outline attachment	*Area coverage*	*Scaffold integrity*
Unchanged (5)	Unchanged (5)	Unchanged (5)
<25% (4)	<75-100% (4)	Minor deformities unrelated to fixation (4)
25-50% (3)	50-75% (3)	Minor cracks close to fixation site (3)
50-75% (2)	25-50% (2)	Fissures that jeopardize the fixation (2)
75-100% (1)	<25% (1)	Fissures and scaffold disorganization in outer area (1)
100% (0)	0% (0)	Fissures and scaffold disorganization in general (0)

	AFG	*PCL*
Outline attachment	1.7 ± 1.50	4.8 ± 0.41
Area coverage	2.7 ± 2.06	4.8 ± 0.41
Scaffold integrity	2 ± 1.79	4 ± 0
Total score	6.3 ± 5.12	13.7 ± 0.82*

Scores show the difference between AFG and PCL efficacy in fixation. AFG shows high variability in results; overall efficacy for fixation with PCL was significantly higher than with AFG (*$p < 0.05$). AFG, autologous fibrin glue; PCL,polycaprolactone.

WORLD VETERINARY ASSOCIATION

3. Modelo de la tuberosidad coxal del equino “in vivo” para estudios de regeneración de hueso y su aplicación al hueso subcondral.

Long term in vivo performance of low temperature 3D printed bioceramics in an equine model. Rafael Vindas Bolaños, Miguel Castilho, Janny de Grauw, Stefan Cokelaere, Saskia Plomp, Jürgen Groll, P. René van Weeren, Uwe Gbureck, Jos Malda. (2019).

Orthotopic bone regeneration within 3D printed bioceramic scaffolds with region-dependent porosity gradients in an equine model. Paweena Diloksumpan, Rafael Vindas Bolaños, Stefan Cokelaere, Behdad Pouran, Janny de Grauw, Mattie van Rijen, Saskia Plomp, P. René van Weeren, Riccardo Levato, Jos Malda. (2019).

Long term in vivo performance of low temperature 3D printed bioceramics in an equine model

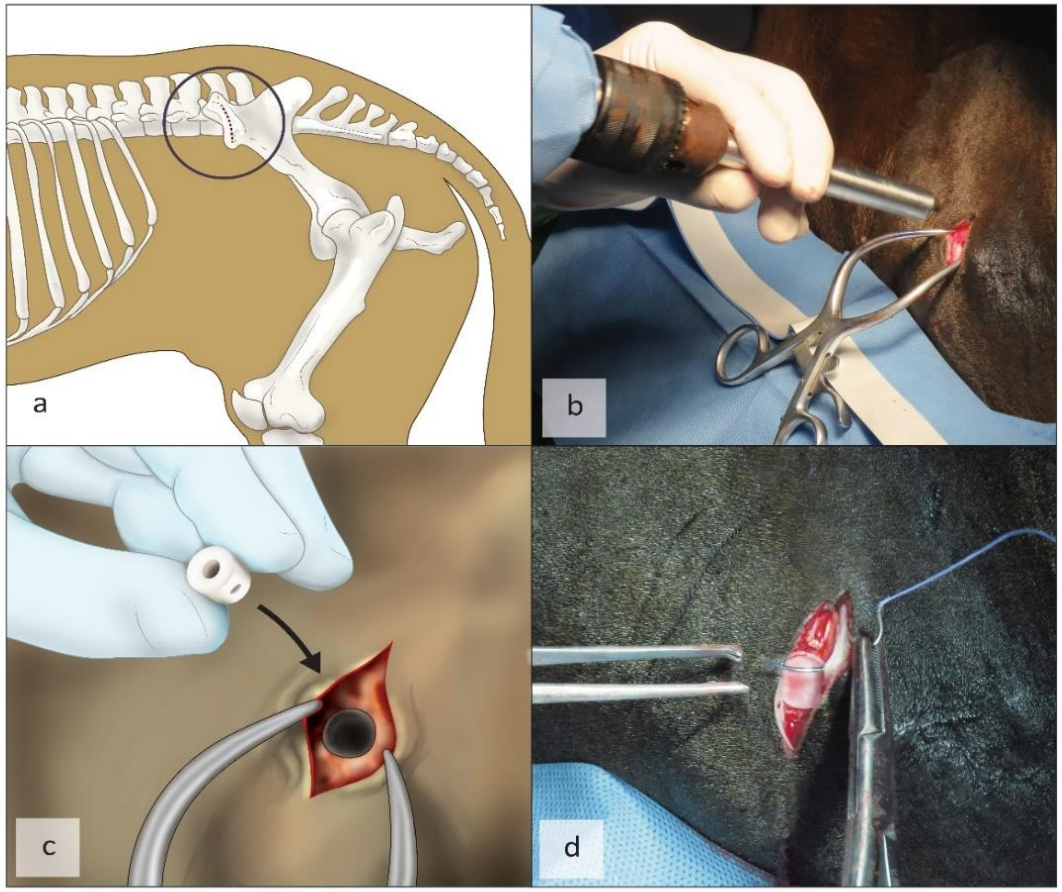

Surgical implantation of 3D printed ceramic implants in the tuber coxae model. A) Position of the tuber coxae of the ileum wing in the horse, B) The defect was made using a power drill, C), Schematic drawing of placement of the scaffold into the defect D) Wound closure.

Long term in vivo performance of low temperature 3D printed bioceramics in an equine model

A) Empty defect

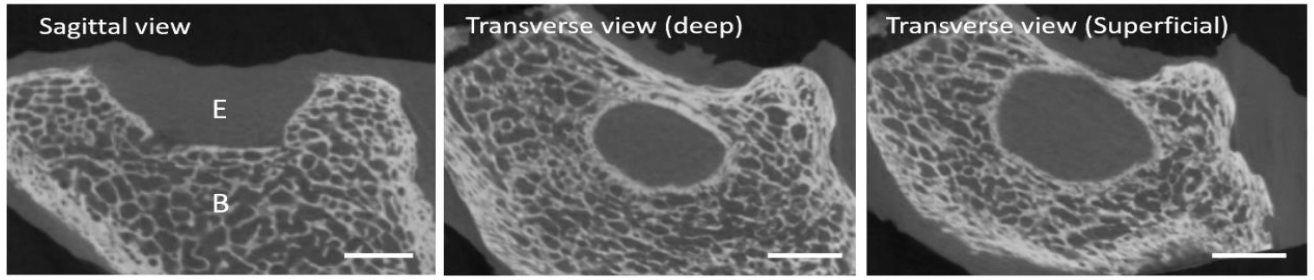

B) Implant after 6months

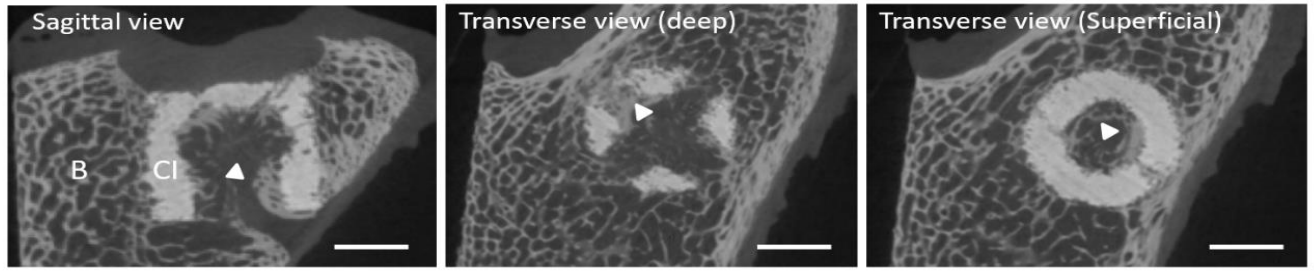

C) Quantification of implant volume after 6months

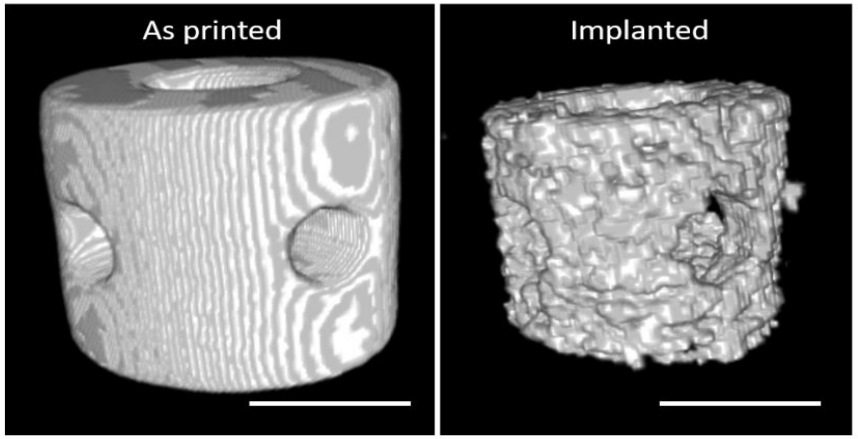

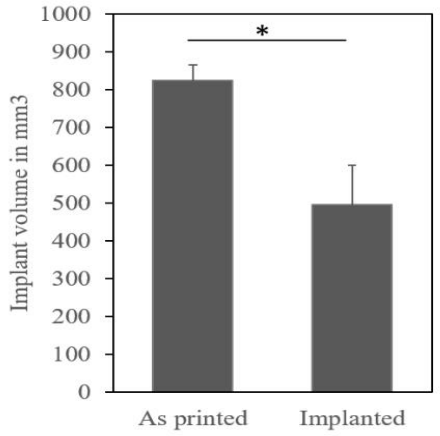

WORLD VETERINARY ASSOCIATION

Orthotopic bone regeneration within 3D printed bioceramic scaffolds with region-dependent porosity gradients in an equine model

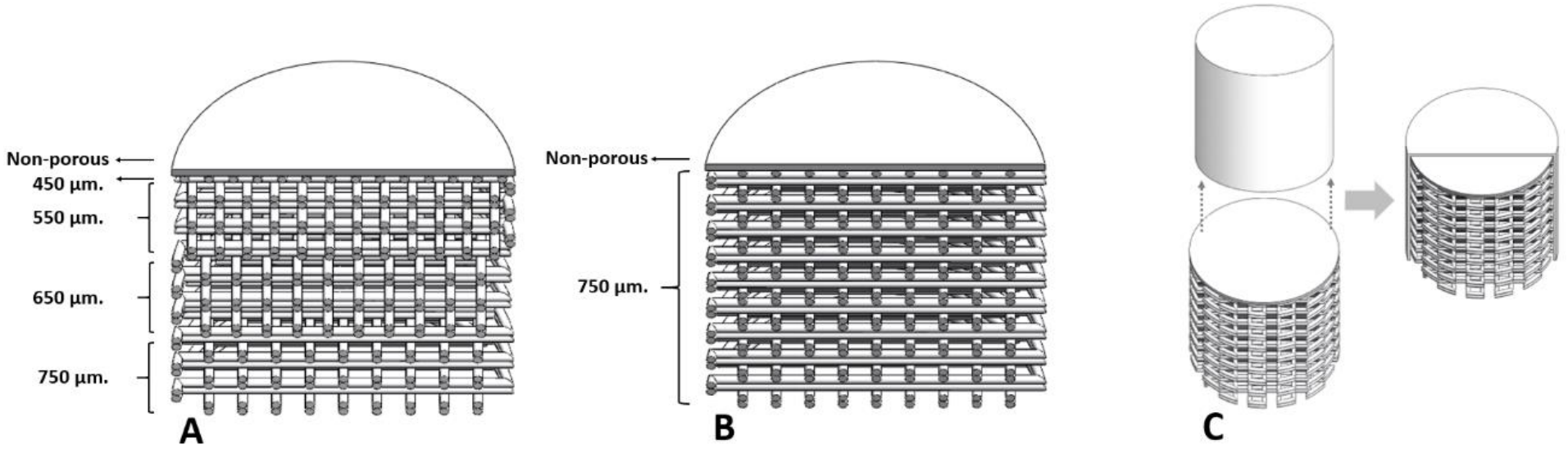

Schematic pictures displaying the cross-section of the PCaP scaffolds with **(A)** gradient and **(B)** constant pore architecture. **(C)** Representation of the PCL-encased PCaP scaffolds.

Orthotopic bone regeneration within 3D printed bioceramic scaffolds with region-dependent porosity gradients in an equine model

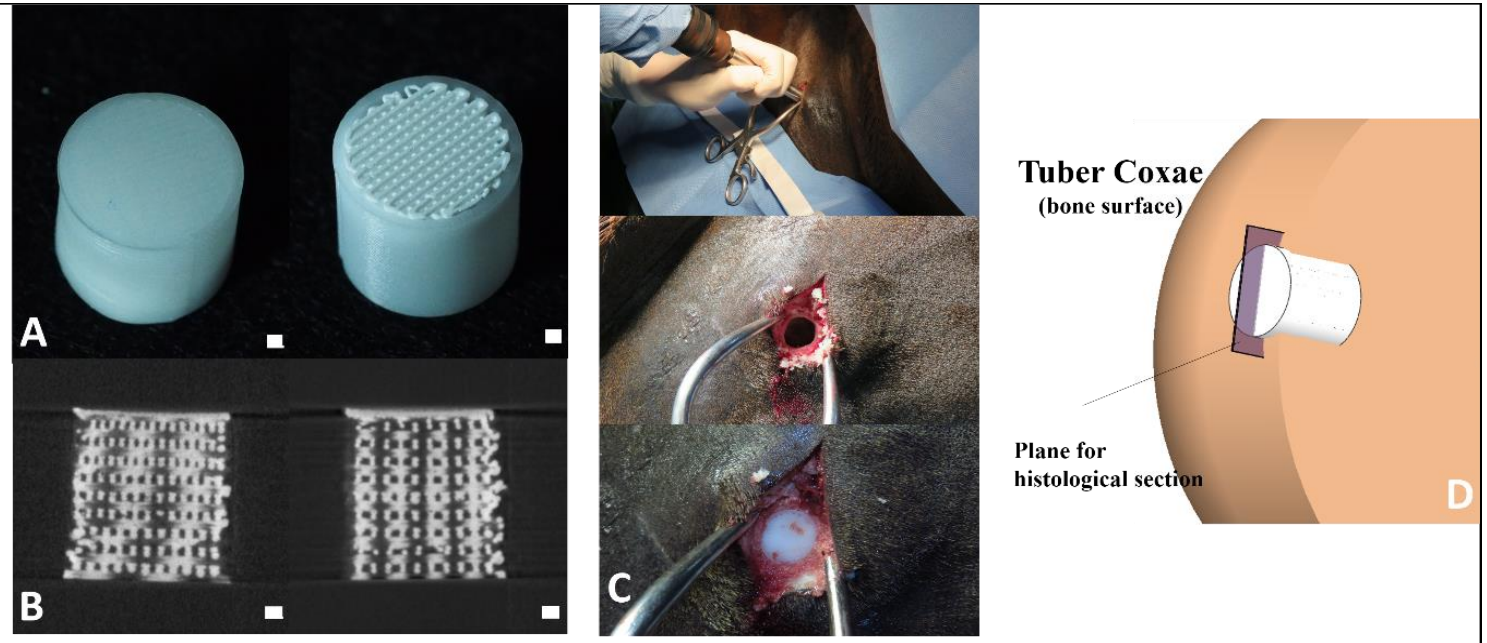

Visualization of the implant and surgical implantation procedure. **(A)** Top (*left*) and bottom (*right*) view of the PCaP implants embedded into the PCL shell. **(B)** Representative µ-CT images of an implant with gradient pore size (*left*) and constant pore size (*right*) before implantation. **(C)** Sequence of implantation of the scaffolds in the tuber coxae, including drilling and exposure of the defect, followed by scaffold implantation. **(D)** Schematic representation of the implant location in the coxal tuberosity. Scale bar = 1mm.

Orthotopic bone regeneration within 3D printed bioceramic scaffolds with region-dependent porosity gradients in an equine model

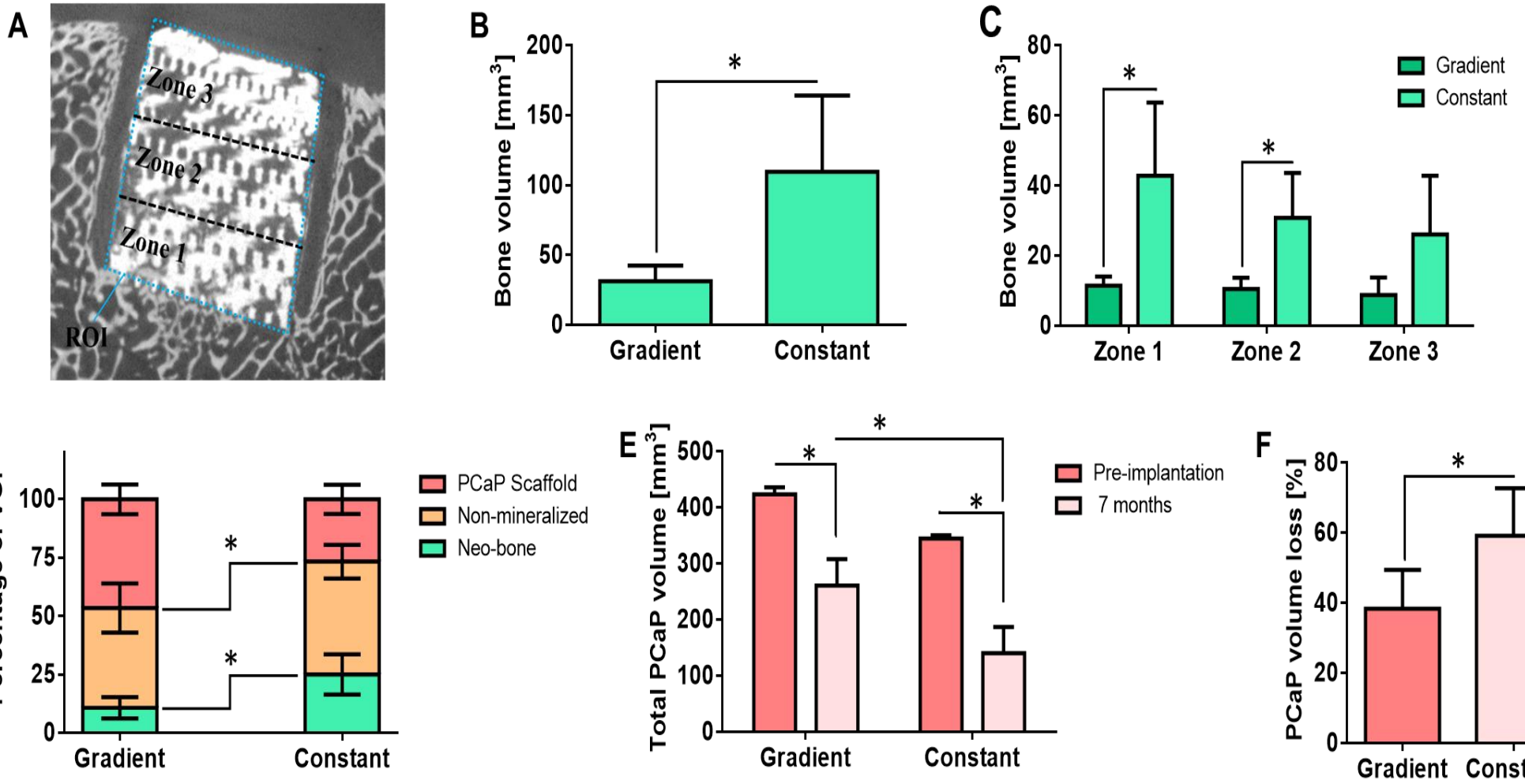

Orthotopic bone regeneration within 3D printed bioceramic scaffolds with region-dependent porosity gradients in an equine model

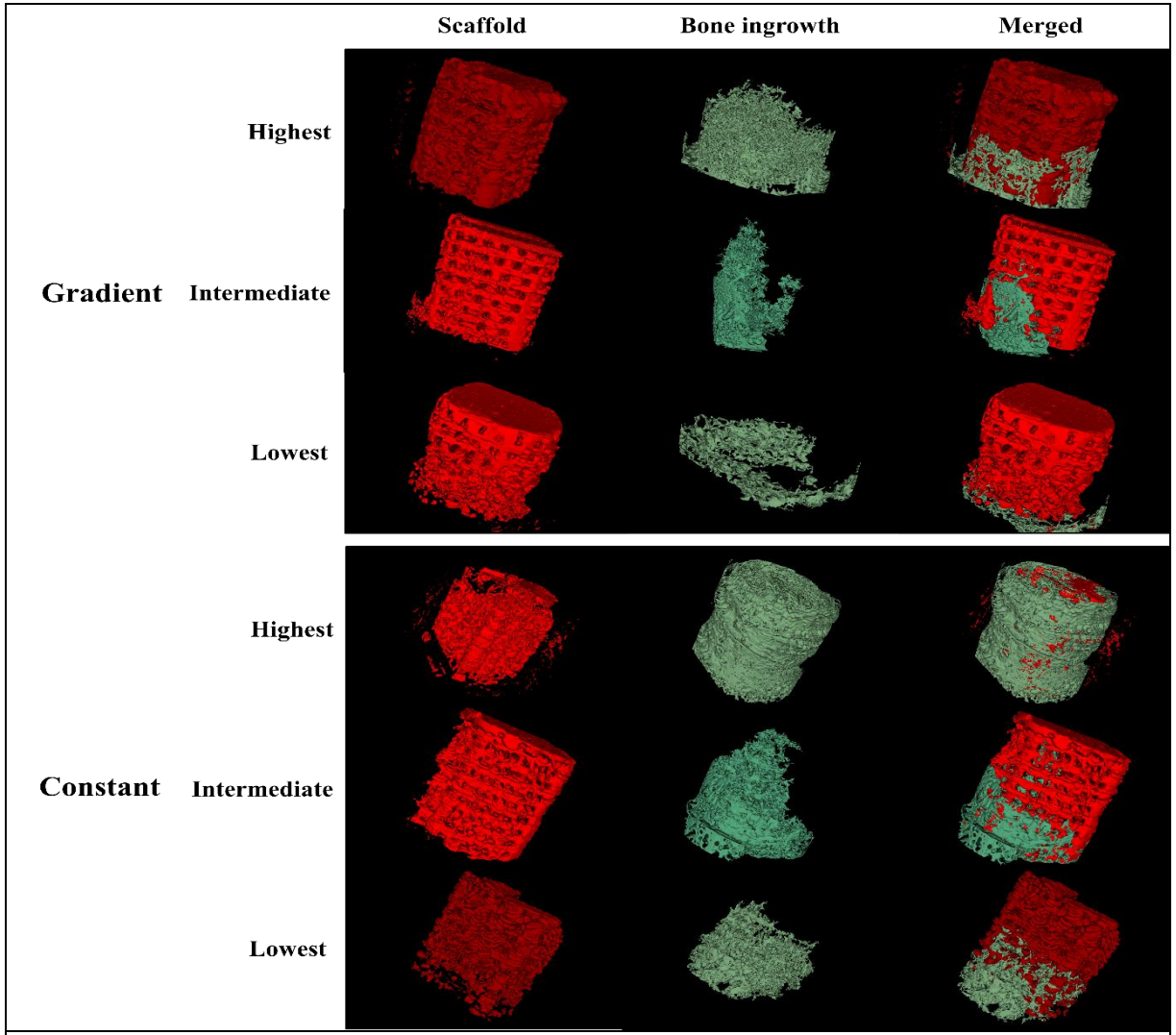

Representative μ-CT 3D reconstruction of the samples with highest, average and lowest new bone formation in scaffolds with gradient and constant porosity.

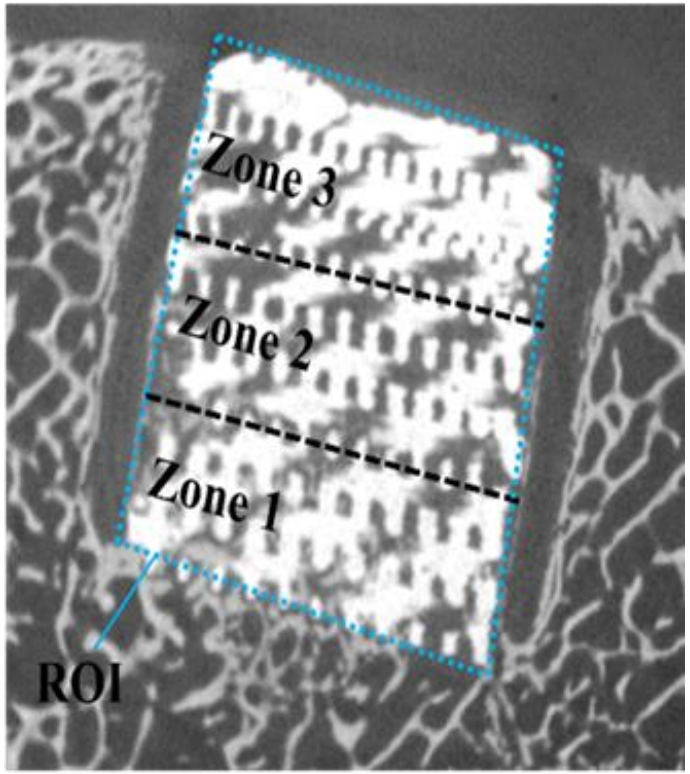

Staining	Structure	Zone 1	Zone 2	Zone 3
TRAP	Gradient	++	++	+++
	Constant	+	++	++
Osteonectin	Gradient	+++	++	+
	Constant	+++	+++	+++
Collagen I	Gradient	+	+	0/+
	Constant	++	++	++

Orthotopic bone regeneration within 3D printed bioceramic scaffolds with region-dependent porosity gradients in an equine model

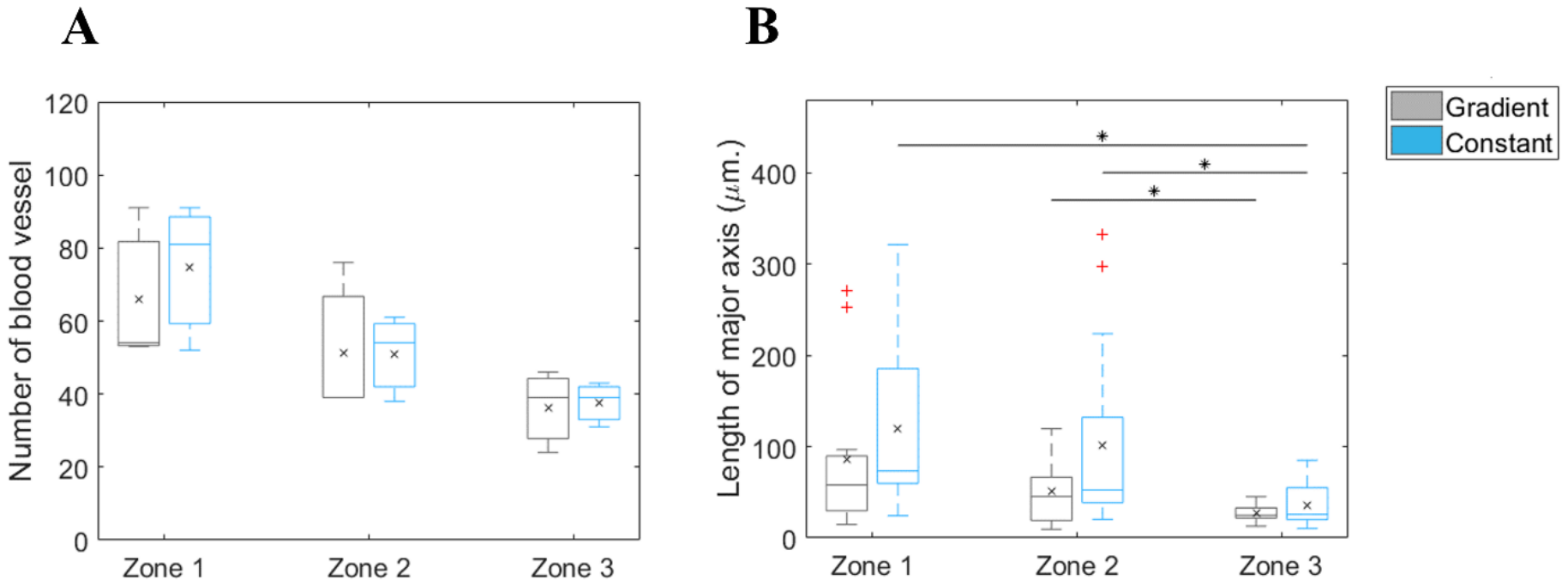

Fig 7: (A) Quantity of blood vessels in each zone. (**B)** Dimension of blood vessels in each zone based on length of the major axis. black x = average, red + = outliers

4. Modelo de la rodilla del equino para estudios de regeneración de cartílago y hueso subcondral mediante defectos subcondrales.

The use of a cartilage decellularized matrix scaffold for the repair of osteochondral defects: the importance of long-term studies in a large animal model. Vindas Bolaños, R.A., Cokelaere, S.M., Estrada McDermott, J.M., Benders, K.E.M., Gbureck, U., Plomp, S.G.M., Weinans, H., Groll, J., van Weeren, P.R., Malda, J. Osteoarthritis and Cartilage, 25, 413-420. (2017).

The use of a cartilage decellularized matrix scaffold for the repair of osteochondral defects: the importance of long-term studies in a large animal model

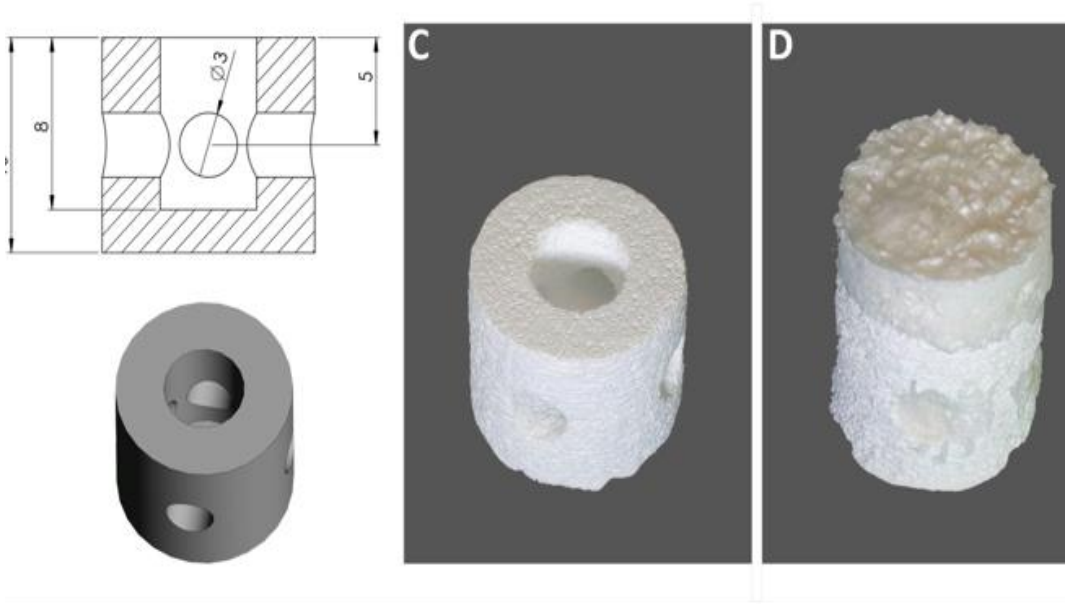

Macroscopic views of scaffolds. The 3D design (A; all distances in mm), rendering (B) and printed CaP scaffold (C), which was subsequently combined in a mould with the CDM scaffold (D).

The use of a cartilage decellularized matrix scaffold for the repair of osteochondral defects: the importance of long-term studies in a large animal model

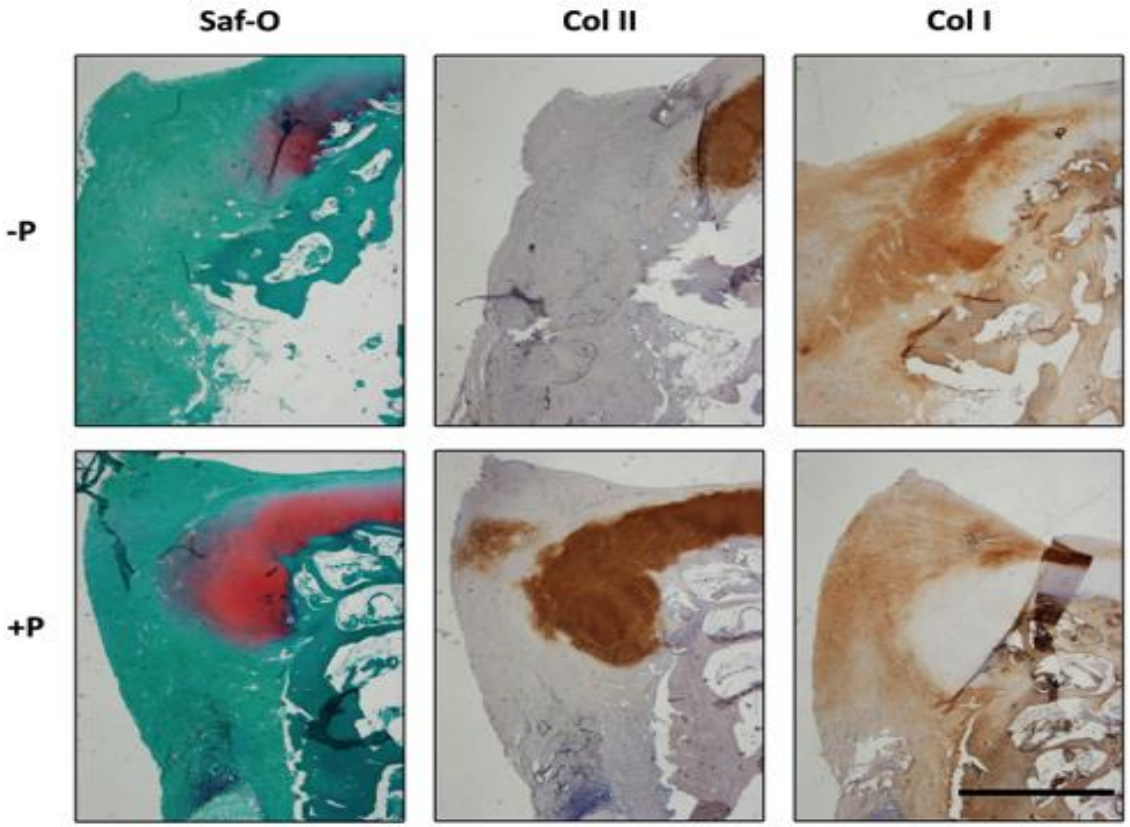

Histological evaluation of the composition of the repair tissue after 6 months. Positive safranin-O staining (red) was predominantly observed at the edges of the defect, and co-localized with the immunolocalisation of collagen type II (brown). Immunolocalisation of collagen type I (brown) was homogeneous in the fibrous repair tissue. Scale bar represents 2 mm.

5. Comparación entre un método de estimulación de la médula ósea y de un novedoso hidrogel auto-adherible en defectos condrales de la rodilla del equino (in vivo) para estudios de regeneración de cartílago.

Technical note - Nanofracturing as a new needling technique for bone marrow stimulation in equine cartilage repair. Stefan M. Cokelaere, Rafael A. Vindas Bolaños, Sanne K. Both, Mariëlle Vullers, Nicoline M. Korthagen, Janny C. de Grauw, P. René van Weeren. (2019).

Use of a self-sealing hydrogel for chondral defects of articular cartilage: a long-term follow-up study in an equine chondral defect model (2019)

Technical note - Nanofracturing as a new needling technique for bone marrow stimulation in equine cartilage repair (2019)

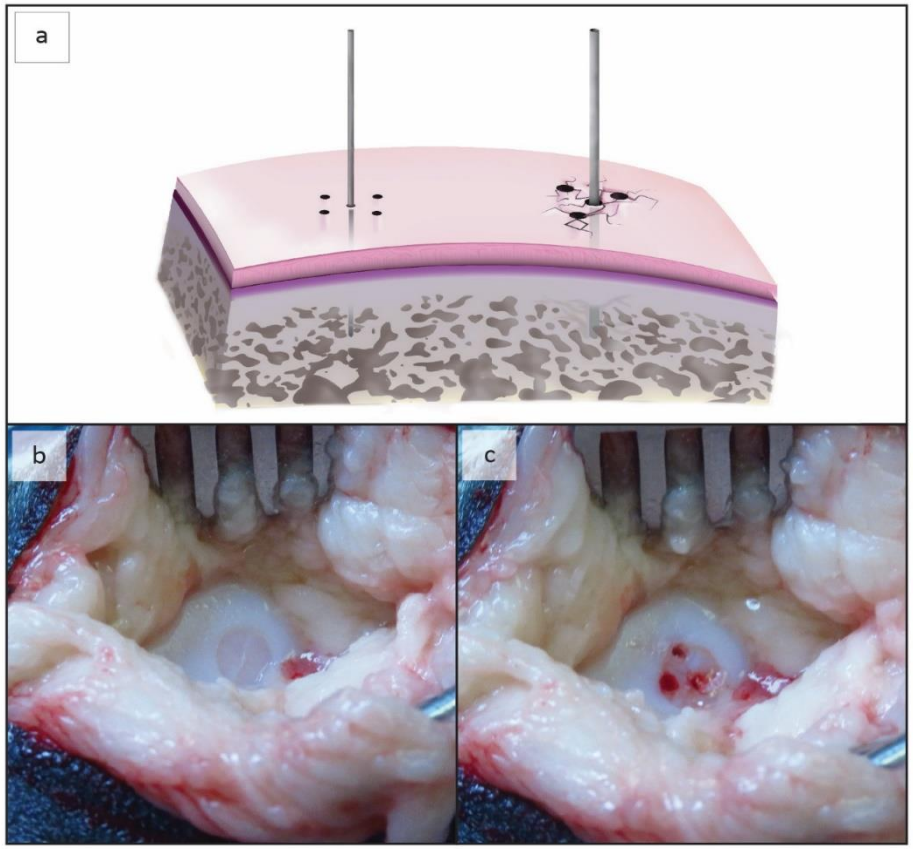

(a) Schematic diagram of nanofracture (left) compared to microfracture (right), showing more adjacent tissue compaction and the wider awl causing more subchondral bone damage with the latter technique (b) photograph of a freshly created partial thickness cartilage defect (c) the same defect after nanofracture was applied.

La nanofractura como una nueva técnica de estimulación de la médula ósea en la reparación de cartílago.

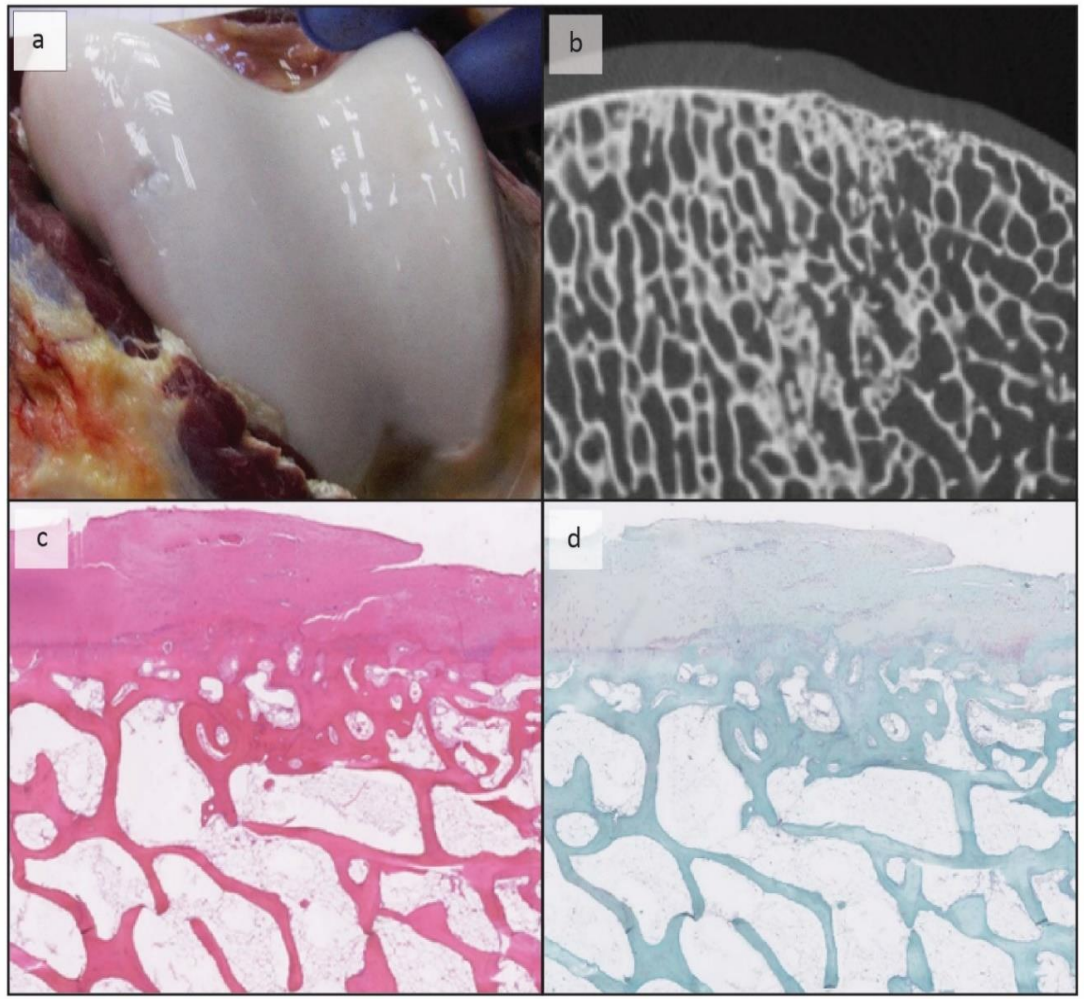

(a) Typical macroscopic outcome 7 months after nanofracture treatment of a surgically created partial thickness cartilage defect on the medial femoral trochlea of a horse (b) MicroCT image of the same nanofracture treated defect 7 months after surgery, revealing mild distiurbance of subchondral bone microarchitecture where surgical perforations were made (c) Image of Hematoxyllin-Eosin (HE) stained section of the same nanofracture treated defect 7 months postoperatively, showing abundant repair tissue with good basal integration but relatively poor cell morphology, tidemark disturbance and mild subchondral bone changes underlying the defect (d) Image of Safranin-O stained section of the same nanofracture treated defect 7 months postoperatively, showing poor cartilage matrix staining.

Use of a self-sealing hydrogel for chondral defects of articular cartilage: a long-term follow-up study in an equine chondral defect model (2019)

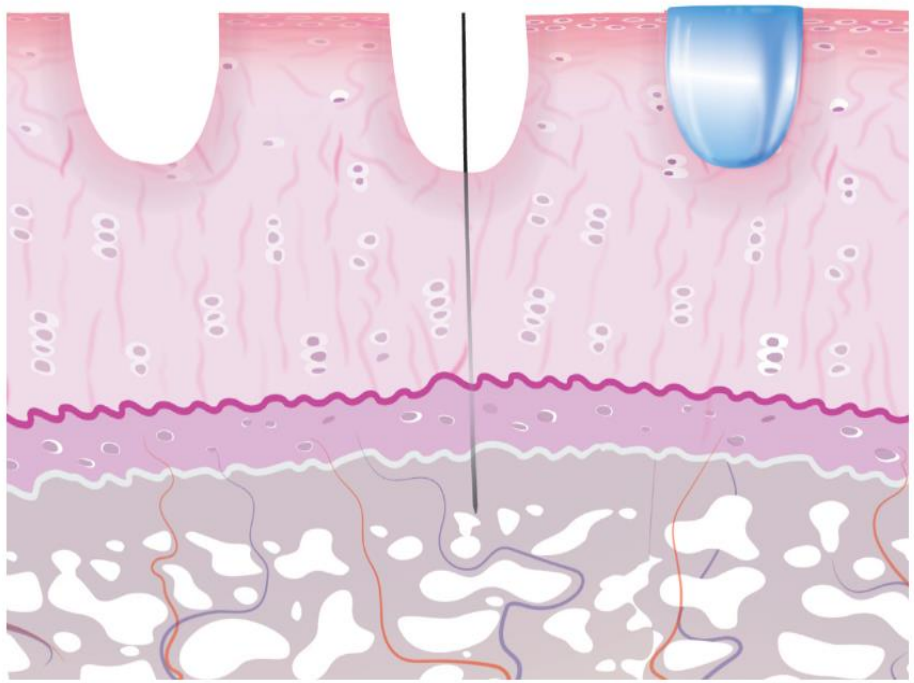

Schematic diagram of surgically created partial cartilage thickness defects before treatment (left), treated with nanofracture, penetrating the subchondral bone plate to engage bone marrow stem cells and trophic factors (middle), or treated with an experimental self-sealing hydrogel that covalently binds to the defect walls and leaves the underlying bone intact (right).

Use of a self-sealing hydrogel for chondral defects of articular cartilage: a long-term follow-up study in an equine chondral defect model (2019)

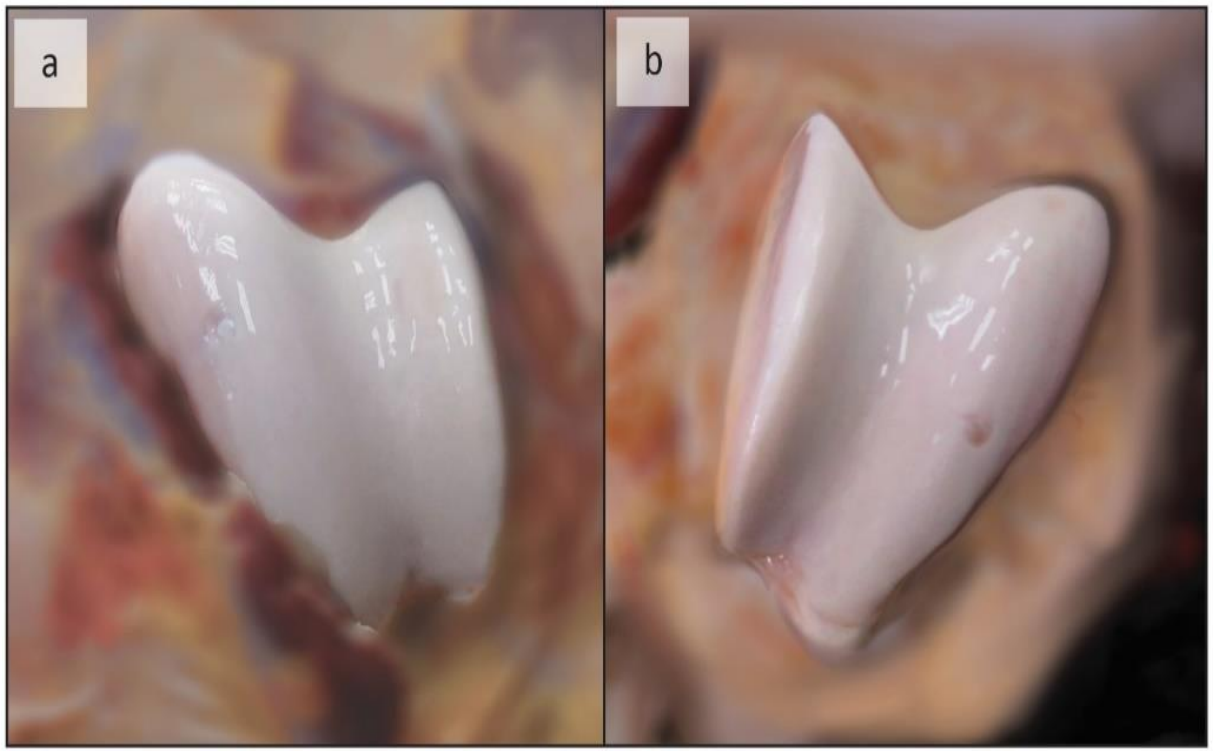

Typical macroscopic appearance of a nanofracture (a) and hydrogel (b) treated partial thickness cartilage defect 7 months after surgical application of either technique in contralateral stifle joints of the same horse. Despite the slightly different camera angle, it can be appreciated that defect location varied by approximately one centimeter between sides.

Use of a self-sealing hydrogel for chondral defects of articular cartilage: a long-term follow-up study in an equine chondral defect model (2019)

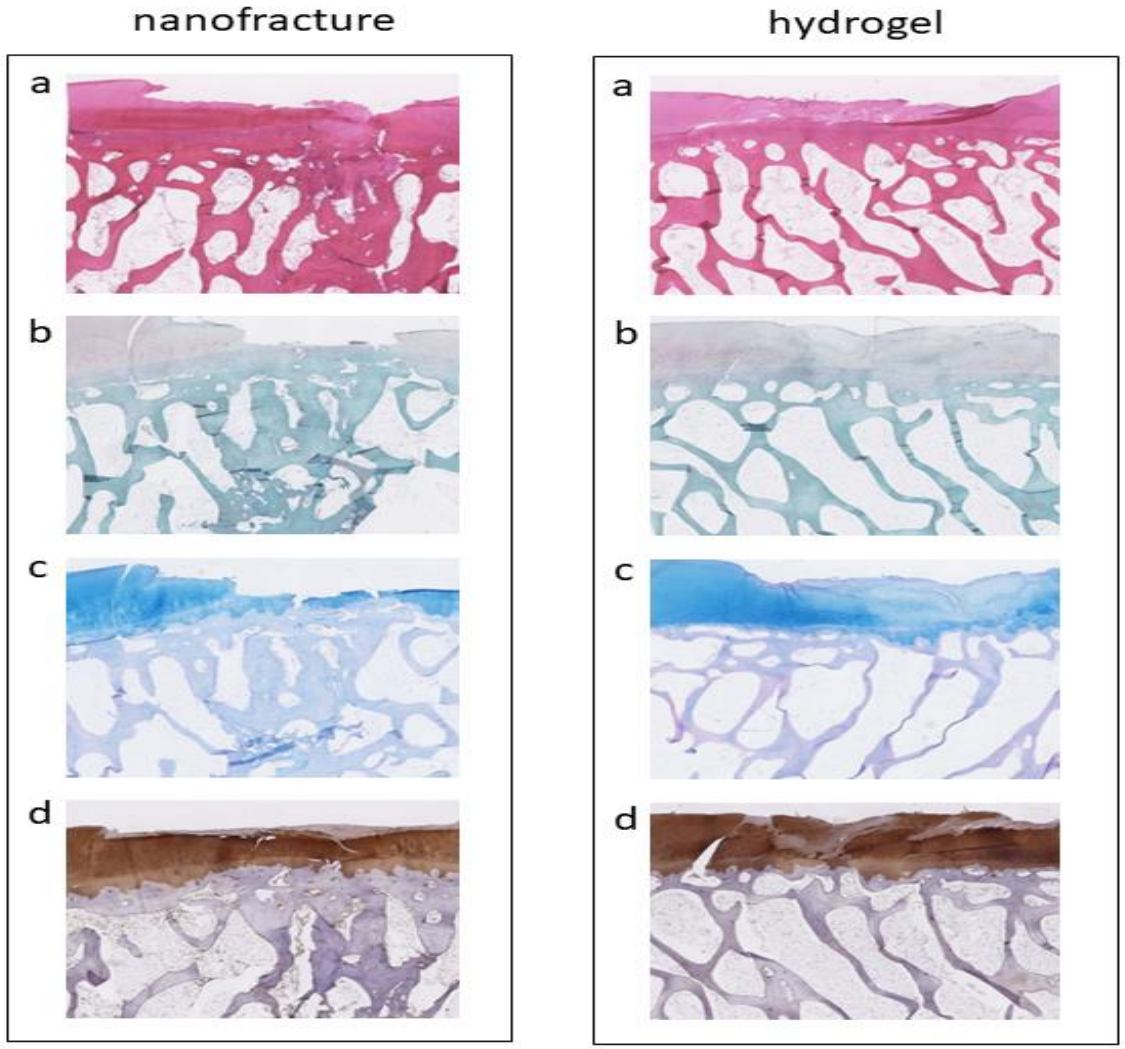

Histological outcome 7 months after nanofracture (left) or hydrogel (right) treatment of partial thickness cartilage defects in contralateral stifle joints of the same horse. (a) Hematoxyllin-Eosin stained section mid-defect (b) Safranin-O stained section mid-defect (c) Alcian Blue stained section mid-defect.

ICRS I Scores: 9 Nanofracture and 5 hydrogel. 12 = Normal repair; 8-11 nearly normal; 4-7 abnormal; 1-3 Severely abnormal.

ICRS II Scores: 48% Nanofracture and 76% Hydrogel. 100% = normal cartilage.

6. Conclusiones y agradecimientos

Conclusiones y agradecimientos

•Los mejor métodos de fijación para estudios de regeneración de cartílago o hueso son: la fijación a presión para defectos osteocondrales (u óseos) y el hidrogel auto adherible para defectos condrales.

•Se utiliza por primera vez el modelo de la tuberosidad coxal del equino como un prometedor modelo para estudios de regeneración de hueso compacto u hueso subcondral.

•La porosidad de los andamios es un factor de relevancia para los estudios de regeneración de hueso, se pudo demostrar que el andamio de porosidad constante de nuestro estudio es más eficiente en la regeneración de tejido óseo que el andamio de porosidad gradual.

•Los estudios de regeneración de hueso y cartílago deben ser a largo plazo (2 años idealmente).

•Se presenta por primera vez la nanofractura como técnica de estimulación de la médula ósea para regeneración o reparación de defectos condrales en la rodilla de equinos y se compara con un novedoso hidrogel autoadherible. Los resultados de ambas investigaciones son prometedores para futuras investigaciones preclínicas y traslacionales.

•Los modelos utilizados en la rodilla y tuberosidad coxal del equino, son de gran utilidad para estudios de medicina regenerativa del equino y además generan información traslacional valiosa para posteriores estudios en humanos.

WORLD VETERINARY ASSOCIATION

Información de Contacto

Email: rafael.vindas.bolaños@una.cr
Teléfono: 83511313

Preguntas y Respuestas